AD-A081 881 STATE UNIV OF NEW YORK AT ALBANY SPACE ASTRONOMY LAB F/G 3/2
BACKGROUND SKY BRIGHTNESS MEASUREMENTS FOR APPLICATION TO SPACE--ETC(U)
FEB 80 J L WEINBERG F49620-78-C-0013

UNCLASSIFIED AFOSR-TR-80-0174 NL

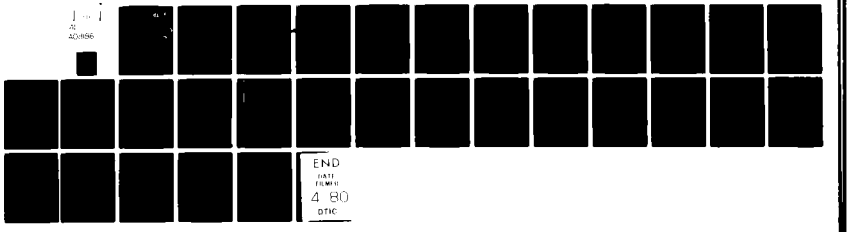

FINAL SCIENTIFIC REPORT

Background Sky Brightness Measurements for Application to Space Surveillance Systems

U.S. Air Force Office of Scientific Research
Contract F49620-78-C-0013
to State University of New York at Albany

1 October 1977 - 30 September 1979

by

J. L. Weinberg
Principal Investigator

Space Astronomy Laboratory
State University of New York at Albany
Executive Park East
Albany, New York 12203

14 February 1980

UNCLASSIFIED

SECURITY CLASSIFICATION OF THIS PAGE (When Data Entered)

REPORT DOCUMENTATION PAGE	READ INSTRUCTIONS BEFORE COMPLETING FORM
1. REPORT NUMBER: AFOSR-TR-80-0174	2. GOVT ACCESSION NO. / 3. RECIPIENT'S CATALOG NUMBER
4. TITLE (and Subtitle): BACKGROUND SKY BRIGHTNESS MEASUREMENTS FOR APPLICATION TO SPACE SURVEILLANCE SYSTEMS,	5. TYPE OF REPORT & PERIOD COVERED: Final rept. 1 Oct '77 - 30 Sep 79
7. AUTHOR(s): J. L. Weinberg	8. CONTRACT OR GRANT NUMBER(s): F49620-78-C-0013
9. PERFORMING ORGANIZATION NAME AND ADDRESS: Space Astronomy Laboratory, State University of New York at Albany, Albany, NY 12203	10. PROGRAM ELEMENT, PROJECT, TASK AREA & WORK UNIT NUMBERS: 61102F 2311 A1
11. CONTROLLING OFFICE NAME AND ADDRESS: AFOSR/NP, Bolling AFB, Bldg. #410, Wash DC 20332	12. REPORT DATE: 14 Feb 80 / 13. NUMBER OF PAGES: 25
14. MONITORING AGENCY NAME & ADDRESS (if different from Controlling Office)	15. SECURITY CLASS. (of this report): unclassified / 15a. DECLASSIFICATION/DOWNGRADING SCHEDULE

16. DISTRIBUTION STATEMENT (of this Report)

Approved for public release;
distribution unlimited.

17. DISTRIBUTION STATEMENT (of the abstract entered in Block 20, if different from Report)

18. SUPPLEMENTARY NOTES

19. KEY WORDS (Continue on reverse side if necessary and identify by block number)

20. ABSTRACT (Continue on reverse side if necessary and identify by block number)

Background starlight has been mapped in blue and red wavelengths over the entire sky, using Pioneer 10 observations from beyond the asteroid belt where the zodiacal light is negligible. Zodiacal light has been isolated in observations between 1 and 3 AU to derive heliocentric dependence. The general solution for inversion of the zodiacal light brightness integral has been derived and is used to yield the scattering function of interplanetary dust for each position traversed by the probe moving through the solar system. Properties of the dust are found to change with heliocentric distance. Polarization of zodiacal light

DD FORM 1 JAN 73 1473 EDITION OF 1 NOV 65 IS OBSOLETE

UNCLASSIFIED 41164

was determined at the north celestial, south ecliptic, and north galactic poles. For inner zodizcal light, symmetry plane of interplanetary dust is close to orbital plane of Venus. At 110 degrees from the sun, it is close to orbital plane of Mars. There appears to be more than one symmetary "plane" for the dust; position of maximum dust density relates closely to orbital planes of the planets. Dust rotation/bursting have been studied as possible important mechanism in comets, interplanetary space, reflection nebulae, stellar envelopes, intersteilar medium. Code has been completed for complete solution to electromagnetic scattering by spheroids. Comparison has been started of observations of Comet 1965 VIII with scattering measurements of irregular particles and with model calculations for sphere, spheroids, and cylinders to derive spatial distribution and physical properties of dust in tail. Zodiacal light polarization observations on antisolar hemisphere contest claim by others that interplanetary dust is aligned and that alignment changes over short times.

Final Scientific Report
AFOSR Contract F49620-78-C-0012

February 1980

Table of Contents

Attachments

Reprint: J. M. Greenberg and D. W. Schuerman, On the Optical Detection of Local Interstellar Particles During an "Out-of-Ecliptic" Mission, Nature, 275, 39-40, 1978.

D. W. Schuerman, Inverting the Zodiacal Light Brightness Integral, Planetary Space Sci., 27, 551-556, 1979.

Reprint: B. A. S. Gustafson and N. Y. Misconi, Streaming of Interstellar Grains in the Solar System, Nature, 282, 276-278, 1979.

Abstracts of (4) papers presented at IAU Symposium 90, Solid Particles in the Solar System, Ottawa, August 1979, Proceedings in press.

Abstract: D. W. Schuerman, The Restricted Three-Body Problem including Radiation Pressure, Astrophys. J., in press.

Space Astronomy Laboratory
State University of New York at Albany

March 1979

Background Sky Brightness Measurements for Application to Space Surveillance Systems

Contract F49620-78-C-0013
U.S. Air Force Office of Scientific Research

Summary

1. Overall objectives and strategy. Studies are made of the brightness, color, and angular distribution of the total diffuse astronomical background radiation and of its components. Ground-based (Mt. Haleakala, Hawaii), Earth-orbital (Skylab), and deep-space probe (Pioneers 10 and 11) observations of zodiacal light (multicolor, brightness and direction and amount of polarization, different times of year and different locations in the solar system, all-sky coverage to within 30° of the sun) are used to derive information on the physical and optical properties of interplanetary dust, its origin and dynamics, its location in space, and its contribution to the infrared astronomical background. In a search for interrelationships, results are compared with meteoritic data, with photometric data on comets, and with properties of interstellar grains.

2. Accomplishments to date. Background starlight has been mapped in blue and red wavelengths over the entire sky, using Pioneer 10 observations from beyond the asteroid belt where the zodiacal light is negligible. Zodiacal light has been isolated in observations between 1 and 3 AU to derive heliocentric dependence. The general solution for inversion of the zodiacal light brightness integral has been derived and is used to yield the scattering function of interplanetary dust for each position traversed by the probe moving through the solar system. Properties of the dust are found to change with heliocentric distance. Polarization of zodiacal light was determined at the north celestial, south ecliptic, and north galactic poles. For inner zodiacal light, symmetry plane of interplanetary dust is close to orbital plane of Venus. At 110° from the sun, it is close to orbital plane of Mars. There appears to be more than one symmetary "plane" for the dust; position of maximum dust density relates closely to orbital planes of the planets. Mini-workshop held in Albany to initiate joint studies of zodiacal light and comet data and interstellar grains. Dust rotation/bursting studied as possible important mechanism in comets, interplanetary space, reflection nebulae, stellar envelopes, interstellar medium. Code completed for complete solution to electromagnetic scattering by spheroids. Started comparison of observations of Comet 1965 VIII with scattering measurements of irregular particles and with model calculations for spheres, spheroids, and cylinders to derive spatial distribution and physical properties of dust in tail. Zodiacal light polarization observations on antisolar hemisphere contest claim by others that interplanetary dust is aligned and that alignment changes over short times. In-house facility completed for digitizing entire library of ground-based observations from Mt. Haleakala, 1964-1968. Night sky observing facility at Mt. Haleakala being reactivated for special purpose observations, near UV to near IR.

Background Information

In October 1976 we began an AFOSR-funded program to complete the reduction and analysis of photometric data from the Pioneer 10/11 deep-space probes and from Skylab and to combine these data with ground-based results and theoretical studies to map the diffuse astronomical background radiation - background starlight and zodiacal light - over the sky and to determine the nature of the interplanetary dust. This report summarizes results obtained through the third year of this program and outlines ongoing tasks in the fourth year, which is supported by Grant AFOSR-80-0043. Additional information is given in the March 1978 Final Report on Grant AFOSR-76-3091 and in the March 1979 Interim Scientific Report on the subject contract.

Summary of Program Objectives, FY 1978-1979

1. To complete the all-sky mapping of Pioneer 10/11 data on background starlight in blue and red wavelengths, using observations from beyond the asteroid belt where the zodiacal light is negligible.
2. To define the brightness of zodiacal light as a function of heliocentric distance, elongation (angular distance from the sun), and ecliptic latitude.
3. To determine the polarization of zodiacal light in the ecliptic and at the north and south celestial, ecliptic, and galactic poles - as a function of heliocentric distance.
4. To establish as far as possible the nature of the particles giving rise to the zodiacal light.
5. To continue the study of electromagnetic scattering by spheroids and cylinders and to compare these results to Mie theory.

In subsequent sections we outline the status of these objectives and of related topics as of the end of FY 1979. We also list papers which were published or are in preparation based on AFOSR support.

Pioneer 10/11 Results

1. Background Starlight. Between March 1972 and February 1976, 76 full or partial sky maps were made by Pioneer 10. Pioneer 11, starting in April 1973, made 67 sky maps. Pioneer 11 was retargeted to encounter Saturn in 1979; Pioneer 10 is continuing on a path that will make it the first probe to leave the solar system. Sky mapping observations from both spacecraft ceased in May 1976. For measurements made between 1 and 2.8 AU, sky maps contain data on background starlight and zodiacal light. Since the zodiacal light was found to be negligible beyond 2.8 AU, these sky maps contain data on background starlight alone. Our procedure was to use merged Pioneer 10/11 background starlight data from a number of maps beyond 2.8 AU to isolate the zodiacal light in maps at smaller heliocentric distances. 98% of the sky is now "mapped" in blue and red wavelengths in a brightness contour format similar to that shown in the March 1978 Final Report on FY 1978 activities. The remaining sky regions have been processed through all but the last step prior to creating final contour plots.

As noted in earlier reports, high resolution maps of the background starlight in several colors are needed to separate the major components of the light of the night sky in observations made from within the zodiacal cloud and are also important from the point of view of knowing the overall topology of the diffuse astronomical background radiation. These maps are also the starting point in the separation and analysis of the background starlight components themselves (integrated starlight, diffuse galactic light, cosmic light).

In response to a number of requests for these data, we have assembled a background starlight data file. This file or data set is composed of 3 parts:

(1) A tabulated matrix in galactic coordinates (b,l) of background starlight in two colors over the sky, in 2-deg increments of b,l.

(2) Contour plots of blue and red brightnesses to the scale of Bečvář's Atlas Coeli. A sample of these data is scheduled for publication in the May 1980 issue of Sky and Telescope.

(3) "Posted" numbers for each field of view data number to construct the contours in (2) above. This allows one to determine the orientation of the Pioneer field of view for each data number over the sky.

With these parts, a user could determine what his instrument would see in absolute units for any size, shape, and field of view orientation - to the Pioneer 10/11 instrument limit of V magnitude~6, which is typical of most large field photometric studies of the diffuse astronomical background radiation. These data are already being provided on a limited basis to the Max-Planck-Institut für Astronomie, Heidelberg, and to the Tokyo Astronomical Observatory. Sample data files were prepared for display and explanation at the Montreal General Assembly of the IAU - for the report of Commission 21's Background Starlight Working Group and for IAU Commissions 28 (Galaxies), 33 (Structure and Dynamics of the Galactic System), 34 (Interstellar Matter and Planetary Nebulae). Based on the large number of requests for these data, we are investigating costs associated with having these data commercially reproduced.

2. Zodiacal Light. All pre-Pioneer 10/11 observations of the zodiacal light yield only the brightness due to the scattering of sunlight by a column density of interplanetary dust. Observations from the Pioneer 10/11 deep-space probes were unique in that the spacecraft could be used as optical

probes. The resulting zodiacal light observations made in the plane of the spacecraft trajectory (approximately, but not exactly, the ecliptic) could be inverted to yield the brightness per unit line of sight as a function of scattering angle. This exact method of inversion (Dumont, Planet. Space Sci., 21, 2149, 1973) was first applied to Pioneer 10 observations as described by Schuerman (Space Research XIX, 447-450, 1979). However, the trajectories of Pioneer 10/11 were not exactly planar as required by Dumont's 2-dimensional inversion formula; the inclinations of the spacecraft orbits varied up to 15^{o} with respect to the ecliptic. We have thus generalized the inversion formula to three dimensions (Schuerman, Planet. Space Sci., 27, 551-556, 1979, attached), and this 3-dimensional inversion methodology has been applied to Pioneer 10 data at 19 heliocentric distances ranging from 1 to 3 AU. Final results were presented at IAU Symposium 90, Solid Particles in the Solar System, Ottawa, August 1979 (abstract attached). Of particular interest is the result that observations from Pioneer 10 do not verify the two major long-standing assumptions: (1) the dust density goes as some power of the heliocentric distance, and (2) the dust properties are independent of location.

An interesting by-product has emerged from our consideration of the symmetry of the interplanetary dust complex. The inversion method mentioned above relies on the assumption of cylindrical symmetary of the dust cloud. In looking for mechanisms which might violate this symmetry, we have derived the general solution for the restricted 3-body problem which includes the effect of radiation pressure on the third (negligible mass) body. The positions of the equilibrium (Lagrangian) points are dramatically altered by radiation pressure; no overabundance of small particles is now expected to be trapped at the L_4 and L_5 points of sun-planet systems. Details of the 3-body problem

with radiation pressure were presented at Ottawa and are in press (abstract attached); certain solutions may be of importance for both solar system dust dynamics and interstellar star formation.

Related Results

- Skylab.

The availability of Pioneer 10/11 all-sky data on background starlight makes it possible to accurately isolate zodiacal light in our Skylab and ground-based observations. The use of this method and these data has resulted in consistently good intercomparisons among our own results and with the results of Dumont and Sanchez. This is especially noteworthy in that the Skylab, Pioneer 10/11, ground, and Dumont and Sanchez measurements were made with completely different instruments, using different techniques of measurement and data reduction and completely independent absolute calibrations.

In this manner, the total and polarized brightnesses and the degree of polarization of zodiacal light were determined for all fixed position Skylab observations: at the north celestial, south ecliptic, and north galactic poles and at 90° from the sun in the ecliptic (vernal equinox); the results were presented at Ottawa (see attached abstract). The same methodology is now being applied to all of the sky-scanning observations obtained from Skylab. The polarization data are reduced in a different manner; they are not affected by background starlight except at low galactic latitudes. Polarization results to date confirm our earlier finding that the directions of polarization of zodiacal light are symmetric with respect to the sun/antisun, with the result that the particles do not have to be aligned.

- Ground-based data.

During the report period existing ground observations continued to be used to provide information on the symmetry plane of the zodiacal cloud. Our results have shown that the symmetry plane is near the orbital plane of Venus at elongations from 32 to 50° from the sun (Misconi and Weinberg, Science, 200, 1484-1485, 1978). Skylab data at 110 to 140° from the sun showed that the symmetry plane is between the orbital plane of Mars and the ecliptic plane at those elongations (Misconi, et al., Bull. AAS, 9, 620, 1977). These results lead us to believe that there is no unique plane of symmetry for the zodiacal cloud, but rather a "multiplicity of planes" associated with the orbital planes of the planets. Additional observational data are needed, especially at elongations beyond 50°. For this purpose we are reactivating our night-sky facility atop 10,000 ft Mt. Haleakala, Maui, Hawaii. The instrument that will be used is a 14-color (near UV to near IR) photoelectric polarimeter with its own alt-azimuth mounting and control and data recording system.

- Digitization of existing ground-based observations.

In the period 1965 to 1968 we made photopolarimetric observations on more than 450 nights. The major portion of these data, and all single-color (5300A) observations dating back to 1961, were recorded in analog (strip-chart) form; funds were not available at that time to acquire and perfect a digital recording system. Approximately 20% of these strip-chart recordings have been digitized using manual techniques, a semi-automatic analog-to-digital chart reader, and a commercially-available digitizing service which utilizes a high speed, laser scanning digitizer (I/O Metrics, Palo Alto, Calif.). These methods are now prohibitive in cost, and we have developed an in-house capability for accurately digitizing these strip-chart recordings. Several

years ago the University acquired a computer-controlled TV camera (EMR Optical Data Digitizer) as the principal ingredient of a digitizing service for University and local research groups. We have refurbished and adapted this digitizer for use with photographic negatives of our strip-chart recordings; the system is now operational, reproducible, and accurate. We are in the process of photographing those recordings bearing directly on the photometric axis of zodiacal light and on other aspects of our current studies.

- Electromagnetic scattering by spheroids.

The complete solution for the scattering of plane electromagnetic waves incident upon homogeneous spheroids was given by Asano and Yamamoto (Applied Optics, 14, 29, 1975). These first solutions contained lengthy and involved mathematics and calculations and were illustrated only for the case of a purely real refractive index. R. Schaefer has worked through the entire mathematics associated with the spheroid, as part of his Ph.D. thesis research at SUNY Albany, and he has extended their original work to include both dielectric and absorbing particles. The computer code was completed and documented during the report period, and a number of particle and ensemble calculations have been made. In studies just completed, excellent agreement was obtained in the first comparison of spheroid calculations with measurements in our microwave analog scattering laboratory.

Additional topics in process include dust rotation/bursting, development of joint (Albany-Leiden-Seoul) studies of zodiacal light and comet data and interstellar grains, the search for color effects in the brightness and polarization of zodiacal light, an observational model of the inner zodiacal light, the reduction of Palomar Sky Survey star count data and their comparison with Pioneer 10/11 background starlight, and models of the diffuse

astronomical background radiation (zodiacal light plus background starlight) at near IR and IR wavelengths.

Contract-related publications and papers presented at meetings

J. L. Weinberg, Summary of Pioneer 10/11 Results on Interplanetary Dust: Zodiacal Light and In Situ, presented at XVI IAU General Assembly, August 1976, Grenoble.

J. L. Weinberg, Light of the Night Sky, Report for IAU Commission 21, in Transactions, IAU, XVI A, Part 1, (ed. G. Contopoulos), 131-139, D. Reidel, Dordrecht-Holland, 1976.

J. G. Sparrow*, J. L. Weinberg, and R. C. Hahn, The 10-Color Gegenschein/ Zodiacal Light Photometer, Applied Optics, 16, 978-982, 1977.

J. L. Weinberg and J. G. Sparrow*, Zodiacal Light as an Indicator of Interplanetary Dust, Chapter 2 in Cosmic Dust, (J. A. M. McDonnell, ed.), 75-122, (New York: John Wiley and Sons), 1978.

J. L. Weinberg, J. G. Sparrow*, R. C. Hahn, and D. E. Beeson, Zodiacal Light Polarization on the Antisolar Hemisphere, Bull. AAS, 8, 502, 1976.

D. W. Schuerman, G. N. Toller, D. E. Beeson, H. Tanabe*, and J. L. Weinberg, Background Starlight at the North and South Celestial, Ecliptic, and Galactic Poles, Bull. AAS, 8, 503, 1976.

N. Y. Misconi, J. L. Weinberg, and D. E. Beeson, Preliminary Results on the Photometric Axis of the Zodiacal Light from Ground-Based Observations, Bull. AAS, 9, 313, 1977.

D. W. Schuerman, J. L. Weinberg, and D. E. Beeson, The Decrease in Zodiacal Light with Heliocentric Distance during Passage of Pioneer 10 through the Asteroid Belt, Bull. AAS, 9, 313, 1977.

J. L. Weinberg and R. C. Hahn, Brightness and Polarization of the Zodiacal Light: Multicolor Results from Skylab, Bull. AAS, 9, 564, 1977.

D. W. Schuerman, The General Inversion of the Zodiacal Light Brightness Integral, Bull. AAS, 9, 564, 1977.

N. Y. Misconi, J. L. Weinberg, R. C. Hahn, and D. E. Beeson, Possible Effects of Mars on the Symmetry Plane of Interplanetary Dust, Bull. AAS, 9, 620, 1977.

D. W. Schuerman, H. Tanabe*, J. L. Weinberg, G. N. Toller, and D. E. Beeson, Two-Color Observations of Background Starlight from Pioneer 10, presented at XXth Plenary Meeting of COSPAR, June 1977, Tel Aviv.

N. Y. Misconi, On the Photometric Axis of the Zodiacal Light, Astronomy and Astrophysics, 61, 497-504, 1977.

N. Y. Misconi and J. L. Weinberg, Is Venus Concentrating Interplanetary Dust to its Orbital Plane?, Science, 200, 1484-1485, 1978.

R. Dumont, M. Rapaport, D. W. Schuerman, and A. C. Levasseur-Regourd, Inversion of the Zodiacal Brightness Integral for an Out-of-Ecliptic Photometer, presented at XXIst Plenary Meeting, COSPAR, June 1978, Innsbruck; Space Research, XIX, 451-454, 1978.

*Visiting Astronomer

Contract-related publications and papers presented at meetings, continued

D. W. Schuerman, The Brightness/Unit Volume of the Zodiacal Light as determined from Pioneer 10, presented at XXIst Plenary Meeting of COSPAR, June 1978, Innsbruck; Space Research, XIX, 447-450, 1979.

J. M. Greenberg and D. W. Schuerman, On the Optical Detection of Local Interstellar Particles during an "Out-of-Ecliptic" Mission, presented at XXIst Plenary Meeting of COSPAR, June 1978, Innsbruck; and Nature, 275, 39-40, 1978.

D. W. Schuerman, Inverting the Zodiacal Light Brightness Integral, Planetary Space Sci., 27, 551-556, 1979.

D. W. Schuerman, Pioneer 10 Observations of the Scattering Function of Interplanetary Dust, Bull. AAS, 10, 613, 1978.

R. Schaefer, Electromagnetic Scattering by Spheroids, Bull. AAS, 10, 614, 1978.

N. Y. Misconi, The Position of the Symmetry Plane of Interplanetary Dust in the Gegenschein, Bull. AAS, 10, 641, 1978.

J. L. Weinberg, and R. C. Hahn, Polarization Reversal in the Zodiacal Light, Bull. AAS, 10, 642, 1978.

B. A. S. Gustafson and N. Y. Misconi, Streaming of Interstellar Grains in the Solar System, Bull. AAS, 10, 653, 1978; and Nature, 282, 276-278, 1979.

Papers Presented at IAU Symposium 90, Solid Particles in the Solar System, Ottawa, August 1979 (to be published in the Proceedings):

N. Y. Misconi, The Symmetry Plane of the Zodiacal Dust Cloud near 1 A.U.

D. W. Schuerman, The Inversion of Pioneer 10 Zodiacal Light Observations.

D. W. Schuerman, The Restricted Three-Body Problem Including Radiation Pressure.

J. L. Weinberg and R. C. Hahn, Brightness and Polarization of the Zodiacal Light: Results of Fixed-Position Observations from Skylab.

D. W. Schuerman, The Restricted Three-Body Problem Including Radiation Pressure, Astrophys. J., in press.

Optical detection of local interstellar particles during an out-of-ecliptic mission

THE contribution to the zodiacal light (ZL) by interstellar grains has been estimated[1-3], but, as suggested here, new observations and analyses of the ZL and of the local interstellar medium provide a firmer basis for placing limits on the brightness of the interstellar (IS) relative to the interplanetary (IP) component. The proposed NASA/ESA 'out-of-ecliptic' (or 'solar polar') mission[4] provides the best and perhaps the only observational method to distinguish between these two components.

To estimate the interstellar dust density, we make the usual assumption that the number density of the interstellar particles (n_{IS}) is related to the local hydrogen number density in the ratio of 10^{-12} (see ref. 5). The local hydrogen density within a few parsecs of the Sun has been observed to be $\sim 0.1\ cm^{-3}$ (ref. 6) which suggests that we are currently passing through an intercloud region of the galaxy. We infer from this gas density that the IS dust content is about $n_{IS} = 10^{-13}\ cm^{-3}$.

The effect of the Solar System on the ambient IS complex of gas and dust is unknown. Although several mechanisms have been proposed either for capture[7,8] or the sweeping out of interstellar grains, none of the results are conclusive because of uncertainties in the basic assumptions. The most efficient mechanism for deflecting interstellar particles (if charged) is probably the Lorentz force exerted by the magnetic field associated with the solar wind[9]. Levy and Jokipii[10] estimate the ratio of the Lorentz to the gravitational force (F_L/F_G) at 1 AU to be 10, but their use of an IS particle size of 0.02 μm is too small by at least a factor of five for the classical size particles[11]. If a realistic particle size of characteristic radius 0.12 μm is used, a value of F_L/F_G of the order of 0.4 (rather than >1) is derived, and sweeping out of the IS particles should not occur. Given the absence of detailed dust orbit calculations as well as the uncertainties in both the initial grain charge properties and in the possibility of the grains discharging in the IP medium, we base our calculations on the assumption that the grains are neither accreted nor swept out, but that the IS grains in the Solar System are uniformly distributed with a density characteristic of the local IS medium.

We estimate the monochromatic IS contribution to the ZL by scattering of solar radiation from an arbitrary distribution of interstellar particles from the brightness integral[12]

$$Z_{IS} = \int_{LOS} f_\odot \left(\frac{R_\odot}{R}\right)^2 n_{IS}(\theta)\, \sigma_{IS}(\theta)\, dl \qquad (1a)$$

which becomes, for a uniform IS density,

$$Z_{IS} = n_{IS} f_\odot R_\odot^2 \int_{LOS} \frac{\sigma_{IS}(\theta)}{R^2}\, dl \qquad (1b)$$

where LOS is line-of-sight, $f_\odot(R_\odot/R)^2$ is the solar flux on a typical volume element at a heliocentric distance R, θ is the scattering angle, $\sigma_{IS}(\theta)$ is the differential scattering cross section of the IS dust, and dl is measured along the LOS. The integral in equation (1b) is calculated from

$$\int_{LOS} \frac{\sigma_{IS}}{R^2}(\theta)\, dl = \frac{1}{b}\int_\epsilon^\pi \frac{F(\theta)}{k^2}\, d\theta \qquad (2)$$

where b is the closest solar approach of the LOS, ϵ is the elongation angle (see Fig. 1), and k is the wave number ($2\pi/\lambda$) of the incident radiation. For the scattering function $F(\theta)$, we use a dielectric dust model[13]. At a wavelength of 4,400 Å, the conversion of cgs radiance units to the unit $S_{10}(V)$ (using the observational parameters recommended by Sparrow and Weinberg[14]) is

$$S_{10}(V) = 1.2\times 10^{-9}\ erg\ cm^{-2}\ s^{-1}\ sr^{-1}\ Å^{-1} \qquad (3)$$

where $S_{10}(V)$ is defined as the radiance produced by a 10th visual magnitude solar (G2V) star per square degree.

According to the model shown in Fig. 1, at the Earth (b = 1 AU and for $\epsilon = 90°$), the IS contribution to the ZL is only about 1 $S_{10}(V)$. This value is not only below the limit of detectability of $\sim 2-3\ S_{10}(V)$ (ref. 15); it is also totally masked by the 200 $S_{10}(V)$ contributed by the IP particles. On the other hand, viewing sunwards from a space craft (located at R = 1 AU) along an LOS parallel to the ecliptic plane and 1/2 AU above it (out-of-the-ecliptic), the IS brightness estimated from equation (2) for the then appropriate value of $\epsilon = 27°$ is $\sim 28\ S_{10}(V)$ which is well above the limit of detectability. Furthermore, this IS contribution may be distinguishable from the IP component.

An observational upper limit to the IS brightness component is established by noting that the ZL is close to solar colour from about 2,200 Å to 2.4 μm (ref. 16 and refs therein). Since the IS particle scattering is colour (wavelength) dependent in this range, this may be used to establish an upper limit to the IS component. Our calculations are confined to the wavelength spread of the UBV system where more data are available for separating the ZL and the background starlight. The ZL in this wavelength region is known to be solar colour to within about 5%.

Assume that the ZL consists of two components, the IP part which is solar colour and the IS component whose wavelength dependence follows the IS dust model previously cited. Thus if we consider the two wavelengths 5,400 Å and 3,600 Å, the IP component has a spectral ratio $I_{IP}(5,400)/I_{IP}(3,600) = 1 (I_{IP} \neq I_{IP}(\lambda)$; I is normalised to solar colour). According to Greenberg and Hanner[13], the IS component has a spectral ratio $I_{IS}(5,400)/I_{IS}(3,600) = 0.77$ at $\epsilon = 90°$.

The 5% colour variation constraint then implies

$$\frac{I_{IP}+I_{IS}(3,600)}{I_{IP}+I_{IS}(5,400)} = \frac{1+I_{IS}(3,600)/I_{IP}}{1+0.77\times I_{IS}(3,600)/I_{IP}} \leq 1.05 \qquad (4a)$$

so that $$\frac{I_{IS}}{I_{IP}}(3,600) \leq 0.25 \quad \text{or} \quad \frac{I_{IS}}{I_{ZL}} \leq 0.20 \qquad (4b)$$

This means that no more than about 20% of the total zodiacal light as viewed in the ecliptic and at 90° elongation can be produced by scattering off of interstellar type particles.

Fig. 1 Resulting ZL brightness in S_{10} (V) units per unit (AU) distance of closest solar approach along the line of sight from $\theta = \epsilon$ to $\theta = \pi$. Inset shows appropriate geometry.

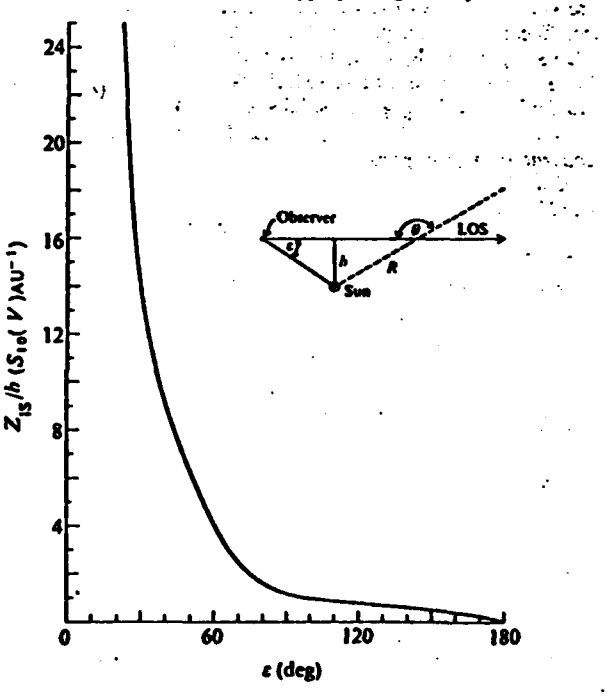

0028-0836/78/0275—0039$01.00

As knowledge of the size and spatial distribution of the IP particles out of the ecliptic is lacking, we derive the maximum amount of IP dust $\frac{1}{2}$ AU off the ecliptic that would still allow the IS component to be distinguished. Let $f \cdot n_{IP}$ be this amount, where n_{IP} is the dust density in the neighbourhood of the Earth and f is the fraction to be determined. As a reference point, the neighbourhood of the Earth has a volumetric scattering cross section of $n_{IP}\,\sigma_{IP}(90°) = 7.8\times10^{-23}$ cm^{-1} sr^{-1} (ref. 17). For $\theta = 45°$, the scattering cross section $\sigma_{IP}(45°)$ is about 1.77 $\sigma_{IP}(90°)$ (ref. 18).

Our minimum distinguishability criterion is that the ratio of the interstellar to interplanetary contributions be greater than 25%. For the case treated above for the interstellar contribution at $\frac{1}{2}$ AU above the ecliptic, then

$$\frac{Z_{IS}}{Z_{IP}} \approx \frac{n_{IS}\sigma_{IS}(45°)}{n_{IP}\sigma_{IP}(45°)} = \frac{7.5\times10^{-11}\times10^{-13}}{f\times1.77\times7.8\times10^{-23}} \geq 0.25$$

from which we obtain $f \leq 0.20$.

This value of f is close to but smaller than those derived from a series of models by Giese[19] which produced results consistent with those inferred from observations from the Earth. Most of these models predict the dust density (assumed to be purely interplanetary) to decrease to 20% between heights of 0.5 and 1 AU above (or below) the ecliptic.

These rough calculations suggest there is a real possibility of optically detecting a local IS dust component in the Solar System. Although our criterion of distinguishability is based on colour arguments alone, both polarisation and scattering angle dependence provide additional tools to distinguish between the larger (IP) and smaller (IS) particles. The chance of isolating the IS component increases with decreasing elongation angle. Observations shoud be made along a line of sight which is parallel to the ecliptic and is as close to the Sun as possible. Fortunately, such observations can also be inverted; not only can the total brightness (Z) be obtained, but when the spacecraft is near maximum height the value $n\sigma$ can be directly determined from the measurements[20].

Assuming that a positive identification of interstellr dust will be made, we are on the threshold of observing physical parameters of these particles which could previously only be inferred from observations of stellar extinction and scattering in reflection nebula, which are normally hundreds of parsecs from our local neighbourhood. For example, given a slightly more optimistic estimate (by perhaps a factor of 2) of the local interstellar dust density, we might be able to observe how they are affected by interaction within the Solar System.

D. S. acknowledges the support of NASA and the US Air Force Office of Scientific Research. We thank Dr R. H. Giese and Dr J. L. Weinberg for useful suggestions.

J. MAYO GREENBERG

Laboratory Astrophysics, Leiden University, The Netherlands

D. W. SCHUERMAN

Space Astronomy Laboratory, State University of New York at Albany.

Received 19 June; accepted 14 July 1978.

1. Öpik, E. *J. Proc. R. Irish Acad.* 54A, 165 (1951).
2. Greenberg, J. M. *Space Res.* 9, 445 (1969).
3. Lillie, C. F. *The Scientific Results from OA002*, (ed. Code, A. O.) 95 (NASA SP-311, 1972).
4. Fisk, L. A. & Axford, W. I. (eds) *Proc. Symp. Study of the Sun and Interplanetary Medium in Three Dimensions* (NASA Publ. X-660-75-53, 1976).
5. Greenberg, J. M. in *Cosmic Dust*, (ed. McDonnell, J. A. M.) chap. 4, 187 (Wiley, London, 1978).
6. McLintock, W., Henry, R. C., Moos, H. W. & Linsky, J. L. *Astrophys. J. Lett.* 204, L103 (1976).
7. Lyttleton, R. A. *The Comets and Their Origin* (Cambridge University Press, 1953).
8. Gary, G. A. *The Contribution of Interstellar Particles to the Interplanetary Dust Complex*, (NASA Tech. Mem., NAS TM X-73377, 1977).
9. Greenberg, J. M. *Proc. IAU Colloq.* No. 13 (1973).
10. Levy, E. H. & Jokipii, J. R. *Nature* 264, 424 (1976).
11. Greenberg, J. M. & Hong, S. S. *Eslab Symp.* No. 8, Fascati (ed. Moorwood, A. F. M.) (ESRO SP 105, 153, 1974).
12. Leinert, C. *Space Sci. Rev.* 18, 281 (1975).
13. Greenberg, J. M. & Hanner, M. S. *Astrophys. J.* 161, 947 (1970).
14. Sparrow, J. G. & Weinberg, J. L. *Lecture Notes in Physics*, No. 48, 41, (Springer, Heidelberg, 1976).
15. Schuerman, D. W., Weinberg, J. L. & Beeson, D. E. *Bull. Am. Astr. Soc.* 9, 313 (1977).
16. Weinberg, J. L. & Sparrow, J. G. in *Cosmic Dust* (ed. McDonnell, J. A. M.) (Wiley, London, 1978).
17. Dumont, R. *Planet. Space Sci.* 21, 2149 (1973).
18. Giese, R. H., Weiss, K. Zerull, R. H. & Ono, T. *Astr. Astrophys.* (in the press).
19. Giese, R. H. *Eldo-Cecles/Euro-Cers scient. tech. Rev.* 7, 43 (1975).
20. Schuerman, D. W. *Bull. Am. Astr. Soc.* 9, 564 (1978).

Extent of hot intergalactic gas in the cluster Abell 2218

A SMALL cooling of the microwave background towards the centre of the rich, distant cluster of galaxies Abell 2218 has been detected[1-3]. This decrement has been attributed to the inverse Compton scattering of photons of the background radiation by electrons in a hot intracluster plasma, as predicted by Sunyaev and Zel'dovich[4]. We report here new observations in several different directions towards the cluster which confirm the earlier results and provide an estimate of the extent of the gas.

The new measurements were made during the period February 1977 to May 1978 at the SRC Chilbolton Observatory, and consist of 199 h of observation at points north and south of the Abell cluster centre[5] and 54 h further at that position. As in previous measurements[1,3], these observations were made at prime focus of the 25-m telescope operated at 10.6 GHz, using a twin-beam system with a beam-throw of 15 arc min in azimuth and HPBW of 4.5 arc min. The receiver incorporated a parametric amplifier with noise temperature about 180 K and bandwidth 250 MHz. The experimental method and data-reduction have been described in detail elsewhere[3].

Table 1 shows the coordinates of the positions observed and the temperature decrements measured there. No corrections for the presence of nearby radio sources are needed[6]. The present results are consistent with earlier measurements near dec 66° 20'—as discussed by Birkinshaw, Gull and Northover[3]. The measurement at dec 66° 18' was made to check on the strong detections at 66° 16' and 66° 20' and to furnish another point close to the cluster centre. Its presence leads to an appreciable

Fig. 1 The galaxy strip count, N, in arc min bins and the observed temperature decrement at each point, ΔT, plotted as functions of declination, δ (1950.0 coordinates). The solid line is the ΔT profile of the best-fitting $\gamma = 5/3$, $\xi = -0.15$ atmosphere convolved with the beamshape of the Chilbolton telescope. The linear scale, D, at the distance of the cluster is also marked.

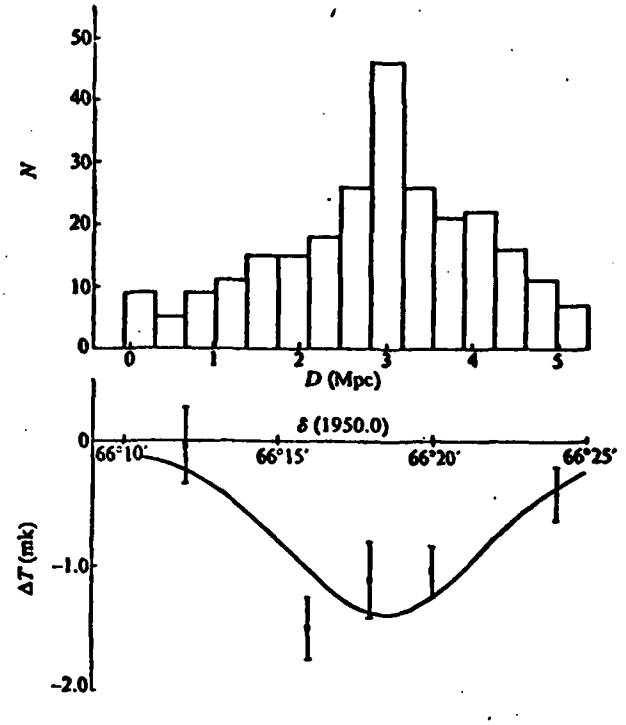

0028-0836/78/0275-0040$01.00

Planet. Space Sci. Vol. 27, pp. 551–556.

0032-0633/79/0401-0551$02.00/0

RESEARCH NOTE

INVERTING THE ZODIACAL LIGHT BRIGHTNESS INTEGRAL

(*Received* 11 *September* 1978)

Abstract—Considerations of the geometry appropriate to observations of the zodiacal light made from out of the ecliptic plane yield the general inversion of the brightness integral. The brightness *per unit volume* of interplanetary space can thus be determined in the immediate neighborhood of the spacecraft in directions confined to a unique viewing plane which depends upon the spacecraft's trajectory. The implementation of this technique guarantees the maximum information content of optical observations made from future deep-space probes including the "Out-of-Ecliptic" mission scheduled for launch in 1983.

1. INTRODUCTION

Measurements of the brightness (Z) and polarization (P) of the zodiacal light represent weighted mean values of the volumetric differential scattering cross-section, $n\sigma_i$, where n is the number density of the dust (cm^{-3}) and σ_i is the cross-section ($cm^2\ sr^{-1}$). The subscript i refers to the two orthogonal components of the scattered radiation. If the electric vector is perpendicular (parallel) to the scattering plane, then $i = \perp (\parallel)$. Each elemental volume of interplanetary space contributes to the brightness along the line-of-sight (LOS) in the amount

$$\zeta_i = \frac{F_\odot R_{ES}^2}{R^2} n\sigma_i \quad (i = \perp, \parallel), \tag{1}$$

where $F_\odot$ is the solar spectral irradiance (ergs $cm^{-2}\ s^{-1}\ Å^{-1}$) at the Earth, R_{ES} is the Earth–Sun distance, and R is the heliocentric distance to the volume element. The total contribution along the LOS is then given by

$$Z = Z_\perp + Z_\parallel = \int_{LOS} (\zeta_\perp + \zeta_\parallel)\, dl, \tag{2}$$

where dl is a small increment of the LOS centered on the elemental volume, and

$$P = \frac{Z_\perp - Z_\parallel}{Z_\perp + Z_\parallel}. \tag{3}$$

(Henceforth, the subscripts denoting polarization will be omitted except when needed for clarity).

The quantity $n\sigma$ or, equivalently, ζ is the most fundamental description of the optical properties of the interplanetary dust complex; no optical measurements of the zodiacal light can yield more information than the spatial, scattering angle (θ) and wavelength dependence of ζ. It is this functional dependence which must be directly compared to light scattering calculations or experimental data to determine the size, shape and index of refraction of interplanetary dust. In lieu of direct determinations of ζ, various assumptions have traditionally been employed to interpret observations of Z and P. The usual practice is to assume that the nature of the interplanetary dust does not depend on its location in the solar system (σ is a function of θ only) and that the spatial distribution of the dust can be represented by a simple law (e.g. $n \propto r^{-a}$ where r is the in-ecliptic heliocentric distance). While this practice gives qualitative insight into the nature of the dust particles, these assumptions, without verification, can introduce misconceptions about the true spatial and scattering angle dependence of $n\sigma$.

Dumont (1973) was the first to point out that deep-space probes could provide a direct determination of ζ, thus removing a major impediment to understanding the nature of the interplanetary dust complex. He developed, on physical grounds, a method of inverting equations (2) and (3) for *zodiacal light observations of* (*and made from within*) *the symmetry plane*. Although not explicitly stated in his paper, his method relies only on the existence of a plane of symmetry for the zodiacal light. Maintaining this assumption here, we treat the general inversion of the brightness integral which can be applied to an observer *arbitrarily located within the solar system* and is particularly appropriate for the "Out-of-Ecliptic" mission scheduled for launch in 1983 (Fisk and Axford, 1976). In the next section, the nomenclature and geometry necessary to evaluate the integrals in equations (2) and (3) are presented. This geometry is used in Section 3 to derive the general mathematical inversion of those equations. In Section 4, the general inversion is applied to a single observer arbitrarily moving through the solar system. The existence of a unique viewing plane is established for which the inversions of equations (2) and (3) are possible. The functional dependence of ζ on scattering angle can then be determined for a range of θ which depends on the spacecraft trajectory.

2. APPROPRIATE GEOMETRY AND EVALUATION OF THE BRIGHTNESS INTEGRAL

Without loss of generality, the ecliptic is chosen as the plane of symmetry. The position of the observer (the point 0 in Fig. 1) is defined by two coordinates, the ecliptic projection (r_0) of the observer's heliocentric distance (R_0) and the observer's height (h_0) above (positive) or below (negative) the ecliptic plane. Thus, $R_0^2 = r_0^2 + h_0^2$, and the angle ψ_0 is defined by $\sin\psi_0 = h_0/R_0$. At the point 0, the direction of the LOS is defined by its ecliptic longitude with respect to the Sun (λ_0') and its ecliptic latitude (β). (The fact that the plane $\beta = 0$ at the point 0 does not contain the Sun should present no confusion. The ecliptic coordinate system is defined on the celestial sphere of arbitrarily large radius, and thus all planes parallel to the ecliptic have $\beta = 0$ whether they contain the sun or not.) The brightness measured at 0 can then be expressed as a function of these four independent coordinates, $Z = Z(r_0, h_0, \lambda_0', \beta)$.

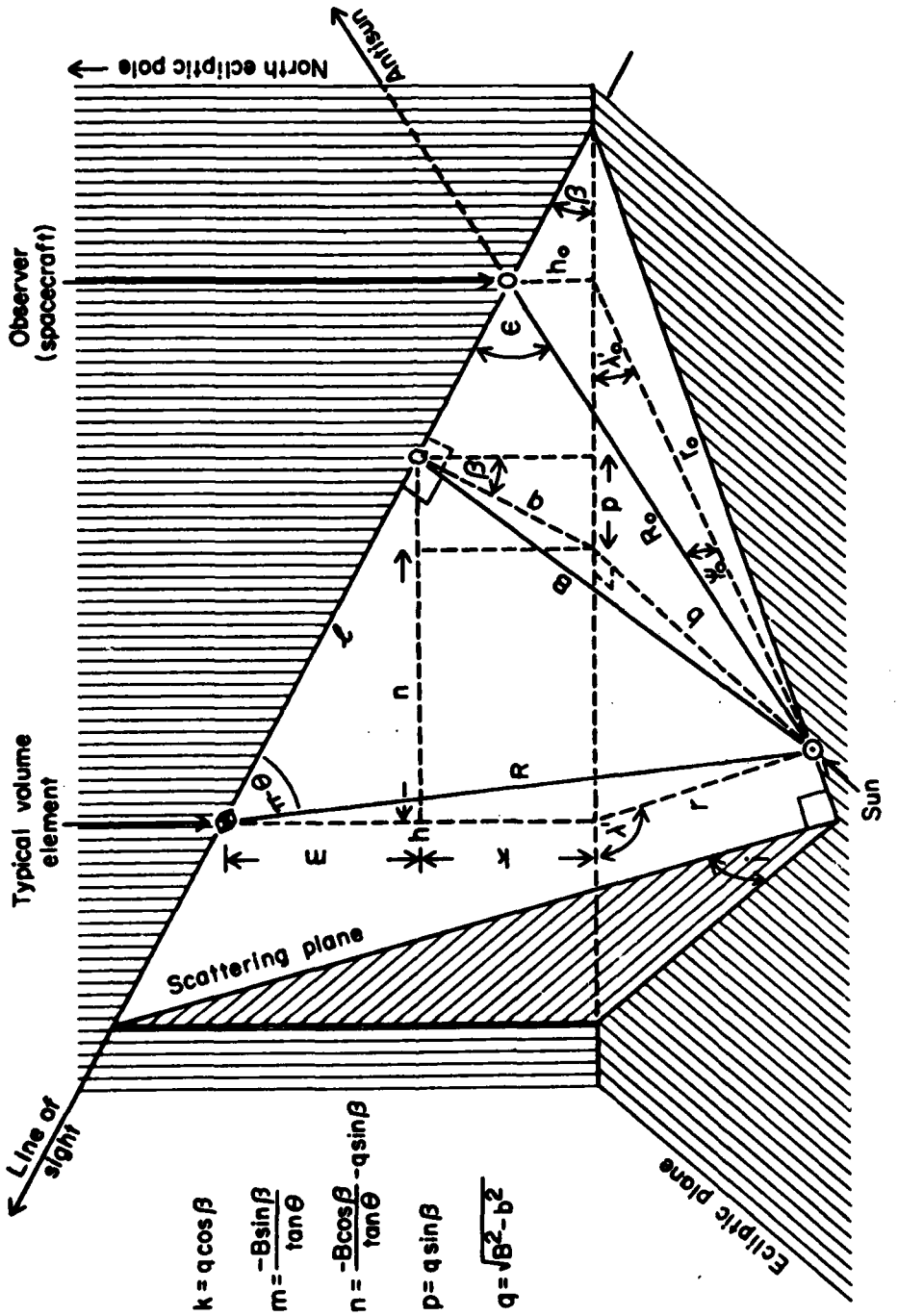

FIG. 1. THE GEOMETRY APPROPRIATE TO OUT-OF-ECLIPTIC ZODIACAL LIGHT OBSERVATIONS.
The scattering plane is defined by the line of sight and the Sun. The point Q is that point on the line of sight which is closest to the Sun. Also shown are all geometric quantities needed to evaluate and to invert the brightness integral.

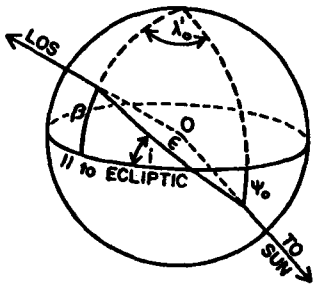

FIG. 2. THE RELATIONSHIP OF THE VARIOUS ANGLES IN FIG. 1 AS DRAWN ON A SPHERE CENTERED ON THE OBSERVER.

Central to this discussion is the expression for the elongation (ϵ), the Sun–observer–LOS angle, in terms of the four independent coordinates. Figure 2 shows the relationship of the various angles as viewed on a sphere centered on the observer. The solution of the spherical triangle, combined with the definition of ψ_0, yields

$$\cos\epsilon = -\frac{h_0}{R_0}\sin\beta + \frac{r_0}{R_0}\cos\beta\cos\lambda'_0. \tag{4}$$

For completeness, we also list the expression for the inclination (i) of the scattering plane with respect to the ecliptic,

$$\cos i = \frac{r_0 \sin\lambda'_0}{R_0 \sin\epsilon}\cos\beta = \frac{b}{B}\cos\beta, \tag{5}$$

where b and B are defined below (Equations 8 and 9).

The brightness seen by an observer at 0 is due to the contribution of all volume elements along the LOS. An arbitrary volume element, as pictured in Fig. 1, is described by its position (r, h) and direction of the LOS (λ', β) in the same manner as was used to describe the position and look direction of the observer, but without subscripts. The scattering angle (analogous to the observer's elongation angle) is defined by the LOS and a line (R) from the sun to the typical volume element. The plane containing these two lines is the scattering plane. Using relationships similar to those used for ϵ, it can be seen that

$$\cos\theta = \frac{-h}{R}\sin\beta + \frac{r}{R}\cos\beta\cos\lambda' \tag{6}$$

and that, for the volume element centered on the observer, $\theta = \epsilon$.

There exist three constants which define any given LOS. The angle β is constant along any such line as are the two lengths designated B and b in Fig. 1. B is the closest solar approach of the line of sight, and b is the same for the projection of the LOS in the ecliptic. (The plane defined by B and b is normal to the LOS at the point Q.) We make extensive use of the fact that, along any given LOS,

$$\beta = \text{constant}, \tag{7}$$

$$b = r_0 \sin\lambda'_0 = r\sin\lambda' = \text{constant}, \tag{8}$$

$$B = R_0\sin\epsilon = R\sin\theta = \text{constant}. \tag{9}$$

Any *point* along the LOS can be parameterized by one other variable. A convenient choice is the scattering angle, θ. Equations (6)–(9) allow r, h, and λ' to be expressed as functions of θ, β, b, and B, the latter three being constant along any given LOS. Explicitly,

$$h = -\frac{B\sin\beta}{\tan\theta} \pm \sqrt{B^2 - b^2}\cos\beta, \tag{10}$$

$$r^2 = h^2 + \left(\frac{B\cos\beta}{\tan\theta} \pm \sqrt{B^2 - b^2}\sin\beta\right)^2, \tag{11}$$

$$\frac{b}{\tan\lambda'} = \frac{B\cos\beta}{\tan\theta} \pm \sqrt{B^2 - b^2}\sin\beta. \tag{12}$$

The geometric relationships expressed by equations (10)–(12) may also be obtained by considering Fig. 1, where $(B^2 - b^2)^{1/2}$ is designated as q. The $+(-)$ sign in the $\pm$ term of equation (10) is used if the point Q is in the northern (southern) ecliptic hemisphere. In equations (11) and (12), the positive sign is used if $\beta > 0$ and Q is in the northern hemisphere or if $\beta < 0$ and Q is in the southern hemisphere; the negative sign is used otherwise.

In evaluating the brightness (2) and polarization (3) integrals, it is convenient to use the scattering angle as the variable of integration. The relations

$$l = \frac{B}{\tan(\pi - \theta)} \quad \text{for} \quad \pi/2 < \theta \le \pi, \tag{13}$$

$$l = \frac{B}{\tan\theta} \quad \text{for} \quad 0 \le \theta \le \pi/2 \tag{14}$$

are used to transform the LOS integration,

$$\int_{l(\theta=\pi/2)}^{l(\theta=\pi)} \frac{dl}{R^2} + \int_{l(\theta=\epsilon)}^{l(\theta=\pi/2)} \frac{dl}{R^2} = \frac{1}{B}\int_{\epsilon}^{\pi} d\theta. \tag{15}$$

(θ is a more convenient variable of integration than is l because the latter has a branch point at $l = 0$, the point Q in Fig. 1). The brightness integral then becomes

$$Z(r_0, h_0, \lambda'_0, \beta) = \frac{1}{B}\int_{\epsilon}^{\pi} (r^2 + h^2)\zeta(r, h, \theta)\, d\theta. \tag{16}$$

The following recipe can now be used to integrate (16). The position (r_0, h_0) of the observer and his choice of the LOS (λ'_0, β) are used to determine β, b, and B via equations (7)–(9). The position of each volume element (r, h) along the line-of-sight can then be specified as a function of θ only (β, b, and B are constant once the LOS is specified) via equations (10) and (11). The integrand in equation (16) is then a function of θ alone, and the evaluation of the integral is straightforward.

3. INVERSION OF THE BRIGHTNESS INTEGRAL

The inversion of the brightness integral is a mathematical description of the simple physical concept pictured schematically in Fig. 3. There, the cumbersome three-dimensional geometry has been restricted to one dimension so that the sun (⊙), the observer (○), and line of sight (→) are embedded in a column of interplanetary material of length $x = L$. The observer, at $x = a$, looks in the antisun direction ($\epsilon = \theta = \pi$) and records a brightness $Z(a)$, as indicated in the figure. The observer then moves a small amount (da) and makes another measurement, $Z(a + da)$. The difference in these measurements, $dZ(a)$,

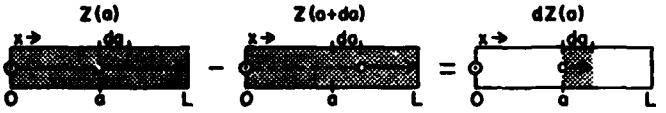

FIG. 3. A SCHEMATIC REPRESENTATION OF THE PHYSICAL MEANING OF INVERTING THE BRIGHTNESS INTEGRAL.

yields information about the material only in the distance interval da, the immediate vicinity of the moving observer. Furthermore, this information depends, not on Z, but upon its derivative, dZ/da.

We now formally apply this technique to equation (16). The act of moving the observer along the LOS corresponds to differentiating the right hand side with respect to ϵ. According to the fundamental theorem of calculus,

$$\frac{1}{B}\frac{d}{d\epsilon}\left[\int_{\epsilon}^{\infty}(r^2+h^2)\zeta(r,h,\theta)\,d\theta\right]=-\frac{R_0^2}{B}\zeta(r_0,h_0,\epsilon=\theta). \tag{17}$$

The left hand side of (16) becomes,

$$\frac{d}{d\epsilon}[Z(r_0,h_0,\lambda_0',\beta)]=\frac{\partial Z}{\partial r_0}\frac{dr_0}{d\epsilon}+\frac{\partial Z}{\partial h_0}\frac{dh_0}{d\epsilon}+\frac{\partial Z}{\partial \lambda_0'}\frac{d\lambda_0'}{d\epsilon}+\frac{\partial Z}{\partial \beta}\frac{d\beta}{d\epsilon}. \tag{18}$$

The total derivatives are geometric quantities which can be evaluated from equations (7), (10), (11) and (12) with h, r, λ' and θ set equal to h_0, r_0, λ_0' and ϵ, respectively. After simplifying the expressions through the use of equations (8) and (9), we find that

$$\frac{dr_0}{d\epsilon}=\frac{-R_0^2}{B}\cos\beta\cos\lambda_0', \tag{19}$$

$$\frac{dh_0}{d\epsilon}=\frac{R_0^2}{B}\sin\beta, \tag{20}$$

$$\frac{d\lambda_0'}{d\epsilon}=\frac{R_0^2}{Br_0}\cos\beta\sin\lambda_0', \tag{21}$$

$$\frac{d\beta}{d\epsilon}=0. \tag{22}$$

The inversion of the brightness integral is therefore given by

$$\zeta(r_0,h_0,\epsilon=0)=-\frac{B}{R_0^2}\frac{dZ}{d\epsilon}\bigg|_{\text{LOS}}$$

$$=\frac{\partial Z}{\partial r_0}\cos\beta\cos\lambda_0'-\frac{\partial Z}{\partial h_0}\sin\beta-\frac{\partial Z}{r_0\,\partial\lambda_0'}\cos\beta\sin\lambda_0'. \tag{23}$$

The polarization per unit volume is obtained by applying equation (23) to each component of Z_i separately and then forming the quantity $(\zeta_\perp-\zeta_\parallel)/\zeta$. For the case $\beta=0$, $h_0=0$, the general solution (23) reduces to the two-dimensional (in-ecliptic) form given by Leinert (1975).

4. APPLICATION TO OUT-OF-ECLIPTIC OBSERVATIONS

The implementation of equation (23) requires the observer(s) to be moving through the solar system. The first statement of the equation formalizes the descriptive argument given at the beginning of Section 3. If the LOS is chosen to be in the direction or antidirection of motion, two measurements of Z separated by an interval $d\epsilon$ along the LOS immediately provide $\zeta(r_0,h_0,\epsilon=\theta)$. Thus, ζ can always be determined for two values of θ (differing by π) at all points along the spacecraft trajectory. The functional dependence of ζ on $\theta(r,h,\lambda',\beta)$ is contained in the second statement of equation (23), but it is not possible for a single spacecraft to measure all three partial derivatives for even a single point in the solar system. A moving observer can, at most, measure the angular derivative and *one* spatial derivative (in the direction of motion). Dumont *et al.* (in press) have demonstrated that those two measurements are sufficient to invert the brightness integral for directions confined to a special viewing plane referred to here as the plane of inversion. This plane limits the range for which the functional dependence of $\zeta(r,h,\theta)$ on θ can be derived from observations. In the mathematical development which follows, the uniqueness of the viewing plane is established and the inversion formula is cast into a form similar to that used for in-ecliptic observations.

Let the unit vector $\bar{s}$ represent a segment of the spacecraft trajectory in the direction of motion; i.e. the spacecraft's instantaneous speed is ds/dt. The plane that contains $\bar{s}$ and the normal to the r,h plane is the plane of inversion. Let ϕ be the angle between the inversion plane and the ecliptic and define a new coordinate system by

$$x=r\cos\phi+h\sin\phi,$$
$$y=-r\sin\phi+h\cos\phi, \tag{24}$$

as shown in Fig. 4. The two spatial derivatives in equation (23) then transform via

$$\frac{\partial Z}{\partial r_0}=\frac{\partial Z}{\partial x_0}\frac{\partial x_0}{\partial r_0}+\frac{\partial Z}{\partial y_0}\frac{\partial y_0}{\partial r_0},$$
$$\frac{\partial Z}{\partial h_0}=\frac{\partial Z}{\partial x_0}\frac{\partial x_0}{\partial h_0}+\frac{\partial Z}{\partial y_0}\frac{\partial y_0}{\partial h_0}, \tag{25}$$

so that

$$\zeta(r_0,h_0,\theta=\epsilon)=\frac{\partial Z}{\partial x_0}(\cos\beta\cos\lambda_0'\cos\phi-\sin\beta\sin\phi)$$
$$-\frac{\partial Z}{\partial y_0}(\cos\beta\cos\lambda_0'\sin\phi+\sin\beta\cos\phi) \tag{26}$$
$$-\frac{\partial Z}{r_0\,\partial\lambda_0'}\cos\beta\sin\lambda_0'.$$

The coefficient of $\partial Z/\partial y_0$ in equation (26) vanishes for those viewing directions in which

$$\cos\lambda_0'=-\frac{\tan\beta}{\tan\phi}. \tag{27}$$

Equation (27) *is the coordinate definition of the plane of inversion.*

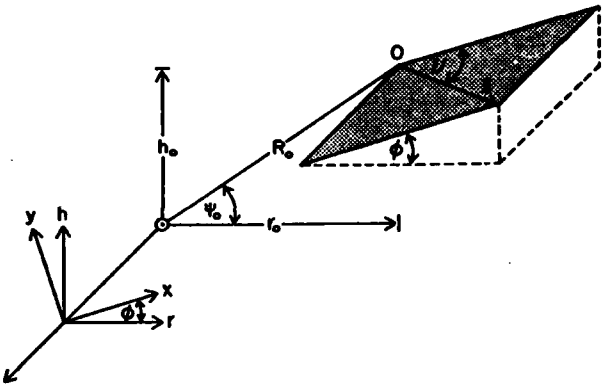

FIG. 4. CONSTRUCTION OF THE INVERSION (SHADED) PLANE; IT IS NORMAL TO THE r, h PLANE AND CONTAINS s, THE DIRECTION OF MOTION OF THE SPACECRAFT.
The angle ϕ is the inclination of the inversion plane with respect to the ecliptic.

For the case of $\phi = 0$, it is obvious from the coefficient of $\partial Z/\partial y_0$ in equation (26) that the inversion plane is parallel to the ecliptic; i.e. $\beta = 0$.

For viewing directions confined to the inversion plane, ζ can be determined without knowledge of $\partial Z/\partial y_0$, provided that $\partial Z/\partial x_0$ and $\partial Z/\partial \lambda_0'$ are known. The angular derivative, $\partial Z/\partial \lambda_0'$, is obtained in practice by scanning across the plane of inversion in *directions parallel to the ecliptic*. The spatial derivative, $\partial Z/\partial x_0$, is obtained by differencing two sets of observations which are separated by a small distance in x, where ∂x_0 is the projection ($x = s \cos \nu$ where ν is measured in the inversion plane as in Fig. 4) of ∂s on the x axis. It is important to recognize that the spacecraft need not be traveling parallel to the x axis in order to determine $\partial Z/\partial x_0$. This partial derivative is a true gradient: the maximum rate of change of Z is along the x axis. Because of the assumption of cylindrical symmetry, this gradient has a zero component in the direction normal to the r, h plane, and its value is immediately determined from increments in Z and x only or by noting that

$$\frac{\partial Z}{\partial s} = \frac{\partial Z}{\partial x_0} \cos \nu. \tag{28}$$

The non-vanishing coefficients in equation (26) have an obvious geometric interpretation as shown on the observer's viewing sphere in Fig. 5. If the angle ξ is measured in the inversion (shaded) plane from the solar meridian to the viewing direction, then the solution of the appropriate spherical triangle in Fig. 5 yields

$$\cos \xi = \cos \beta \cos \lambda_0' \cos \phi - \sin \beta \sin \phi, \tag{29}$$

$$\sin \xi = \cos \beta \sin \lambda_0', \tag{30}$$

and ϵ and ξ are related by

$$\cos \epsilon = \cos \xi \cos (\psi_0 - \phi). \tag{31}$$

These substitutions bring the inversion formula into the simple form

$$\zeta(r_0, h_0, \theta = \epsilon) = \frac{\partial Z}{\partial x_0} \cos \xi - \frac{\partial Z}{r_0 \, \partial \lambda_0'} \sin \xi, \tag{32}$$

which is reminiscent of the in-ecliptic solution and reduces to it ($x_0 = r_0$, $\xi = \lambda_0' = \epsilon$) for $\phi = 0$, $\beta = 0$, $h_0 = 0$. Formula (32) allows ζ to be determined at all points of the solar system encountered by the probe and for all values of the scattering (elongation) angle within the range

$$(\psi_0 - \phi) \le \theta = \epsilon \le \pi - (\psi_0 - \phi). \tag{33}$$

The determination of ζ requires observations to be made in directions other than the inversion plane. The angular derivative in equation (32) can only be obtained from observations which at least straddle this plane. The fact that $\partial Z/\partial \lambda_0'$, rather than $\partial Z/\partial \xi$, appears in equation (32) is due once again to the only crucial assumption inherent in this development, that of cylindrical symmetry.

A very direct check on this sole assumption will be possible during the Out-of-Ecliptic mission. After a gravitational assist by Jupiter, the spacecraft will travel back

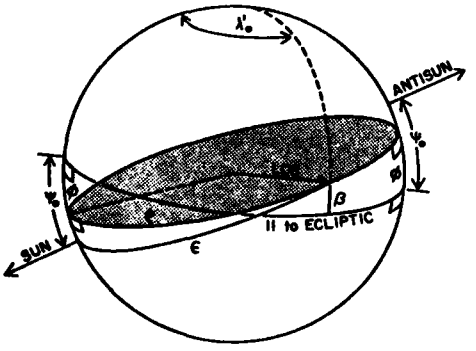

FIG. 5. THE OBSERVER'S VIEWING SPHERE SHOWING THE INVERSION (SHADED) PLANE.

"over" ("under") the Sun. Approximately 3 yr into the mission, solar polar passage will be attained at which time the spacecraft will be near the center of the solar system but approximately 1.6 a.u. above (below) the ecliptic plane. From this vantage point, all isophotes of the brightness of the zodiacal light will be circles centered on the sun if the assumption of cylindrical symmetry is correct. Any long-term influences of the planets on the interplanetary dust complex should also be discernable as changes in the brightness distribtuion near the orbits of the planets.

Acknowledgements—The author wishes to thank Dr. R. Dumont (Observatoire de Bordeaux) for many helpful discussions and for pointing out the existence of the inversion plane on physical grounds. Dr. J. L. Weinberg (SUNY at Albany) brought the problem to the author's attention and provided a critical reading of the manuscript. This work was supported by the Air Force Office of Scientific Research (Contract F49620-78-C-0013) and by the National Aeronautics and Space Administration (JPL Contract 955137).

D. W. Schuerman

Space Astronomy Laboratory,
State University of New York at Albany,
Albany, NY 12203,
U.S.A.

REFERENCES

Dumont, R. (1973). *Planet. Space Sci.* **21**, 2149.
Dumont, R., Rapaport, M., Schuerman, D. W. and Levasseur-Regourd, A. C. *Space Res.* XIX. In press.
Fisk, L. A. and Axford, W. I. (Eds.) (1976). Proceedings of the Symposium on the Study of the Sun and Interplanetary Medium in Three Dimensions. NASA publication X-660-75-53.
Leinert, C. (1975). *Space Sci. Rev.* **18**, 281.

increase in the visual luminosity, with little change in the bolometric luminosity. Outflow velocities will be lower than in classical novae: roughly the same order as the escape velocity from the stellar surface.

Consequently there will be two types of spectroscopic and colour change produced by variations in the accretion rate. In the subcritical regime, increased accretion rates produce increasing disk temperatures along with increasing luminosity—both visual and bolometric. In the supercritical regime the disk is surrounded by an outflowing optically thick wind and the bolometric luminosity is held close to the Eddington value, L_{ed}. Increases in the wind mass-loss rate due to further increased accretion now produce decreasing temperatures along with increasing visual luminosity. The emission line spectrum of the disk will be replaced by an absorption line spectrum formed in the outflowing envelope—similar to the F or A type spectrum observed in classical novae at outburst maximum.

Is there any evidence for this supercritical state? The photographic magnitude of M33 Var A fell by 3.5 mag (ref. 5) in the visual in 1950–52, rose by 1.0 mag in 1952, before finally falling off sharply. Hubble and Sandage note that the changes in colour index indicate that the bolometric luminosity changed by only 1.4 mag. The visual luminosity fell by ~60 while the bolometric luminosity fell by ~4. This agrees with the expected changes due to a variable optically thick wind at Eddington luminosities.

η Carina is a close galactic relative to the Hubble–Sandage variables. It has broad spectral lines, with relatively strong Fe II and [Fe II][6]. Davidson[19] deduced a temperature of 3×10^4 K for the underlying star. Between 1836 and 1856 η Carina underwent a major outburst, followed by a subsidiary outburst in 1889. The early F absorption spectrum of 1893 was slowly replaced by the characteristic emission spectrum. The absolute magnitude at outburst was ~−14 (ref. 20), several magnitudes brighter than normal classical novae. At present, a cool surrounding dust cloud[21] heated by the underlying stellar source produces the bulk of the emission. The bolometric luminosity is still ~−14, but most of the emission is re-radiated IR from the dust shell. This high and constant luminosity, the spectral changes, the broader than average emission lines, and the nova-like explosion indicate that η Carina could contain a massive, main-sequence, accreting component in a binary which underwent a burst of supercritical accretion. Polarisation observations[20] of the nebula suggest that the dust is concentrated in an annulus of size 10^4 AU, and this has been interpreted as evidence of binary structure. This is the first observational indication of possible binary structure in this type of object. A search for binary eclipses in Hubble–Sandage variables with periods in the range weeks to years would test the binary model.

The bright galactic source MWC349 is a similar object[7]. Thompson *et al.*[22] interpret optical and IR observations as a proto-planetary disk seen face-on. In terms of the structure of the luminous source their model closely resembles that described here. The main difference is their interpretation as a preplanetary disk rather than an interacting binary.

If the brightest known optical stars are powered by infall of material on to a main-sequence star, the importance of accretion as an astrophysical energy source would be established beyond its present applications to X-ray binaries, novae and active galactic nuclei and quasars[23]. Such binaries should exist, and they would be classified as Hubble–Sandage variables when observed in external galaxies.

I thank J. Barrow and A. Edwards for helpful comments.

Received 9 July; accepted 18 September 1979.

1. Bath, G. T., Evans, W. D., Papaloizou, J. & Pringle, J. E., *Mon. Not. R. astr. Soc.* 169, 447 (1974).
2. Pringle, J. E. *Mon. Not. R. astr. Soc.* 178, 195 (1977).
3. Pringle, J. E. & Rees, M. J. *Astr. Astrophys.* 21, 1 (1972).
4. Shakura, N. I. & Sunyaev, R. A. *Astr. Astrophys.* 24, 337 (1973).
5. Hubble, E. & Sandage, A. *Astrophys. J.* 118, 353 (1953).
6. Humphreys, R. M. *Astrophys. J.* 200, 426 (1975).
7. Humphreys, R. M. *Astrophys. J.* 219, 445 (1978).
8. Rosino, L. & Bianchini, A. *Astr. Astrophys.* 22, 453 (1973).
9. Warner, B. *IAU Symp.* No. 73, 85 (eds Eggelton, P., Mitton, S. & Whelan, J. A. J.) (Reidel, Dordrecht, 1976).
10. Bath, G. T., Pringle, J. E. & Whelan, J. A. J. *Mon. Not. R. astr. Soc.* (in the press).
11. Kraft, R. P. *Astrophys. J.* 135, 408 (1962).
12. Ulrich, R. K. & Burger, H. L. *Astrophys. J.* 206, 509 (1976).
13. Kippenhahn, R. & Meyer-Hofmeister, E. *Astr. Astrophys.* 54, 539 (1977).
14. Neo, S., Miyaji, S., Nomoto, K. & Sugimoto, D. *Publ. astr. Soc. Jap.* 29, 249 (1977).
15. Schwarzschild, M. & Härm, R. *Astrophys. J.* 128, 348 (1958).
16. Iben, I. *Astrophys. J.* 142, 993 (1965).
17. Stothers, R. *Astrophys. J.* 138, 1074 (1963).
18. Bath, G. T. *Mon. Not. R. astr. Soc.* 182, 35 (1978).
19. Davidson, K. D. *Mon. Not. R. astr. Soc.* 154, 415 (1971).
20. Warren-Smith, R. F., Scarrott, S. M., Murdin, P. & Bingham, R. G. *Mon. Not. R. astr. Soc.* 187, 761 (1979).
21. Pagel, B. E. J. *Astrophys. Lett.* 4, 221 (1969).
22. Thompson, R. I., Strittmatter, P. A., Erickson, E. F., Witteborn, F. C. & Strecker, D. W. *Astrophys. J.* 218, 170 (1977).
23. Lynden-Bell, D. *Nature* 233, 690 (1969).

Streaming of interstellar grains in the Solar System

B. Å. S. Gustafson*† & N. Y. Misconi*

* Space Astronomy Laboratory, State University of New York at Albany, Albany, New York 12203
† Lund Observatory, University of Lund, Sweden

Deep-space probes offer excellent opportunities to study interstellar grains streaming into the Solar System. Direct detection of such particles would considerably add to our knowledge in many areas of cosmic dust research and could also provide information on the characteristics of both the interstellar medium and the interacting solar wind. Here we present the results of a theoretical study of the interaction between interstellar grains and the solar wind, including the effects of solar cycle variations in the interplanetary magnetic field. The latter is shown to influence significantly regions of concentration and depletion of interstellar grains within the Solar System.

Observations of the neutral gas in the solar vicinity suggest that the Solar System is moving relative to the local interstellar matter in a direction ≈7° north of the solar equatorial plane (ecliptic longitude and latitude: $\lambda \simeq 250°$, $\beta \simeq 7°$)[1], and at a speed of ≈20 km s^{-1} (ref. 2). Bertaux and Blamont[3] computed number densities of interstellar grains in the solar cavity taking into account only gravitation and radiation pressure. Of the types of grains used in their model and based on their calculation of β (radiation pressure to gravitational attraction) only 0.02-μm radius silicate grains were able to penetrate deeply inside the Solar System. They estimated the number density of these dust grains to be strongly peaked on a line extending from the Sun backwards in the downstream direction. This number density was found to be higher by a factor of ~100 than direct observations of dust grains by Alvarez[4]. In an attempt to clarify this difference, Levy and Jokipii[5] made an order of magnitude estimate of the Lorentz force exerted by the solar wind magnetic field on a charged grain. They showed that if the 0.02-μm radius silicate grains of Bertaux and Blamont carry a net charge of 5 V, then the Lorentz force strongly dominates, thereby destroying the gravitational focusing and suggesting that these grains are largely excluded from the Solar System.

Studies of interstellar grains suggest two populations of particles[6]: (1) elongated core–mantle particles of characteristic radius ≈0.12 μm, with a ≈0.07 μm radius core of silicate type material, and a rather complex mantle of molecular mixtures of mainly oxygen, carbon and nitrogen; and (2) ≈0.01 μm thick silicate and/or graphite type grains. Bertaux and Blamont did not consider any of these populations. In the following calculations (see also, ref. 13) we show that although population (1) particles have $\beta > 1$, they still penetrate deep inside the Solar System.

The magnitude of the radiation pressure is given by $P_{pr} = (S/c)Q_{pr}$, where S is the flux, c is the speed of light, and Q_{pr} is the radiation pressure efficiency: $Q_{pr} = Q_{abs} + Q_{sca}\ (1 - \langle\cos\theta\rangle)$, where Q_{abs} and Q_{sca} are the efficiency factors for absorption and scattering, respectively, and $\langle\cos\theta\rangle$ is the asymmetry factor over

0028/0836/79/460276—03$01.00

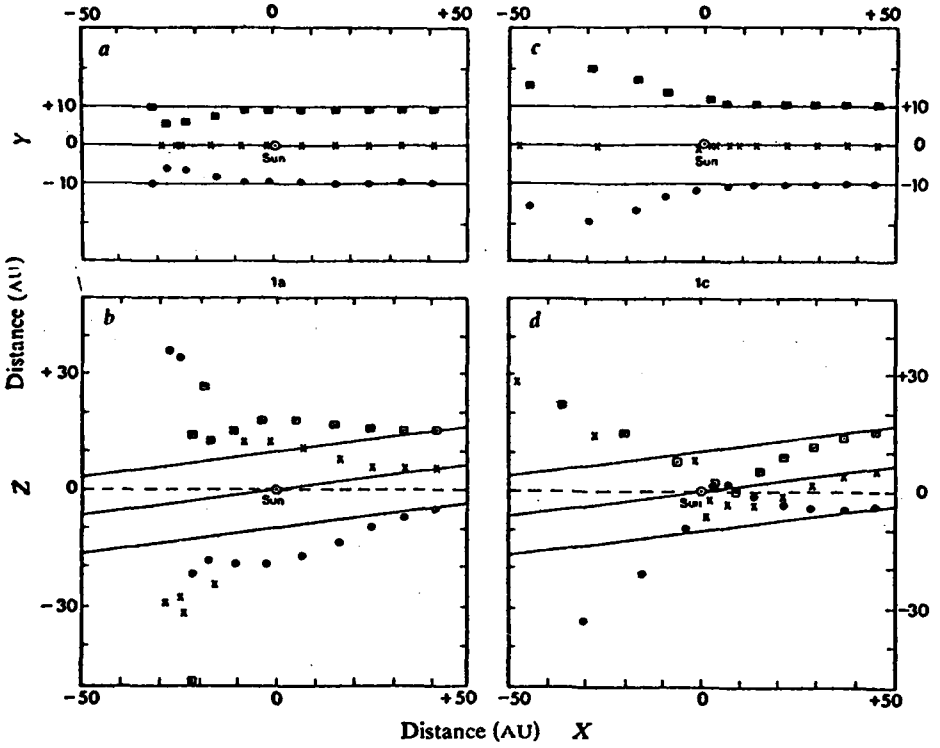

Fig. 1 Instantaneous positions of the 0.12 μm core–mantle particles initially moving in the direction $\lambda = 70°$, $\beta = 7°$ along the solid lines. The particles are entering the Solar System at $X = +50$ AU with 2 yr interval. Three streams (■, ×, ●) introduced at $Z = +6$ AU are projected onto the solar equatorial (X–Y) plane at the beginning (a) and in the middle (c) of a solar magnetic cycle. In b and d the three streams (⊡, ×, ⊙) introduced at $y = 0$ are similarly projected onto a plane (X–Z) perpendicular to the solar equatorial plane (dotted line).

the scattering angle θ. Scattering dominates over absorption for these dielectric particles in the scattering-efficient resonance region, and Q_{pr} was estimated using Mie theory for homogeneous spheres of equal volume and averaged core–mantle index of refraction. For a spherical silicate core coated by a concentric smooth spherical ice mantle representing particles of population (1) the computed Q_{pr} value using this approximation was found to be 0.4 ($\beta = 1.3$). As the grains that penetrate (population (1)) spend 30 yr or less in the Solar System, all radiation forces other than radiation pressure are negligible. Both solar-induced photoelectron emission and the accretion of solar wind ions will tend to charge these grains positively, whereas electron accretion produces negative charge. The equilibrium charge state is given by the relation

$$\sigma_e(V_0)f_e = \sigma_i(V_0)f_i + y\sigma_{ph}f_{ph} \qquad (1)$$

where the σs are the cross-sections of the grains for UV photons, ions and electrons, the fs are the corresponding fluxes, y is the photoelectron yield, and V_0 is the electrical potential of the grains. σ and y have been estimated for numerous silicates, and these lead to charges ranging from 5 to 12 V (refs 7, 8). The photoemission properties are not usually decreased by surface impurities or adsorbed layers[7], or by amorphous structure[8]. However, for ice the work function is near the Lyman edge, and therefore photoemission is less efficient. We will adopt here +7 V for bare particles, and +1.2 V for the core–mantle grains. As the charged grains interact with the solar wind described by Svalgaard *et al.*[9], they will be subject to a Lorentz force given by

$$F_L = \frac{q}{c}[(V_g \times B) - (V_{sw} \times B)] \qquad (2)$$

where q is the grain's charge, V_g and V_{sw} are the speeds of the grain and of the solar wind, respectively, c is the speed of light and B is the magnetic field strength.

The magnetic field is torn in an archimedian spiral by the solar rotation. Thus

$$B_r = \frac{B_0}{r^2} \quad \text{and} \quad B_\Phi = \frac{-B_0\omega b^2(r-b)\sin\theta}{V_{sw}r^2} \qquad (3)$$

where B_0 is the magnetic field strength at some reference distance ($b = 5$–10 solar radii), ω is the solar angular velocity, r is the heliocentric distance, Φ is the azimuth angle, and θ is the heliocentric colatitude angle. The second (electrical) part of equation (2) which acts along θ will dominate as the grains enter the Solar System at low and medium heliocentric latitudes. This force, acting on a grain of given charge, is independent of the speed of a radially streaming solar wind as can be seen by substituting equation (3) in equation (2); high velocity plasma streams will not alter our results considerably.

The positive and negative magnetic fields are separated by a sinusoidal warped neutral sheet[10,11], the amplitude of which we assume to decay exponentially with increasing heliocentric distance. The speed of the solar wind as a function of θ was assumed to be of the form

$$V_{sw} = a + b\,|\cos\theta| \qquad (4)$$

where a is the mean solar wind velocity at the equator (400 km s^{-1}) and b is 300 km s^{-1}.

The grains also encounter other less important forces such as Coulomb drag due to the nearby passing solar wind electrons, which is given by

$$F_C = \frac{\pi s^2 N_e e^2 V_0^2}{m_e W^2} \ln\left(\frac{W^2 m_e P}{e V_0 s}\right) \qquad (5)$$

where s and V_0 are the radius and charge of the grain, respectively, N_e, e, and m_e are the electron number density, charge and mass, respectively, and W is the velocity of the grains relative to the electrons. P is the impact parameter, which is assumed to be $\approx N_e^{1/3}$, following a poissonian distribution for the nearest neighbour distance. Another force is ion pressure resulting from impinging solar wind ions on the grains which is given by

$$F_i = \pi s^2 \bar{M}_i V F \qquad (6)$$

where F is the flux of the solar wind ions, V is their velocity and $\bar{M}_i$ is the mean ion mass $\approx 2 \times 10^{-24}$ g.

Trajectories of interstellar grains streaming into the Solar System were computed as follows: the grains are introduced at the boundary of the solar wind cavity ($X = 50$ AU) at the beginning of the 22-yr solar magnetic cycle (defined as the cycle beginning when the solar dipole field acquires a south component). The equations of motion are integrated at small intervals of time (24 h), and the position, speed and acceleration of the particles are determined.

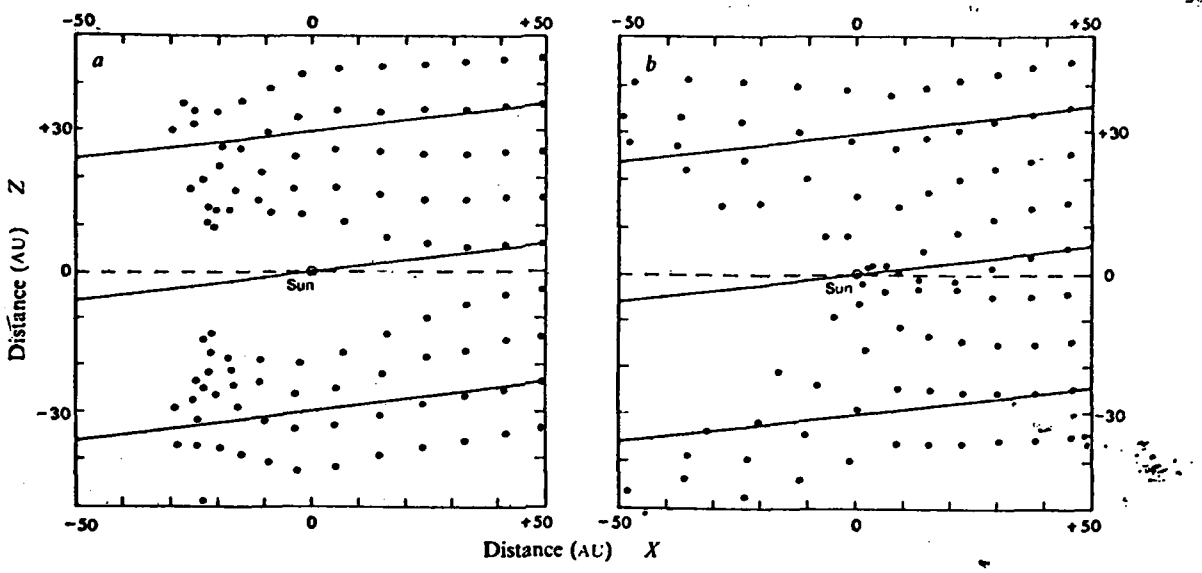

Fig. 2 Instantaneous positions of combined high latitude streams and the streams shown in Fig. 1*b* and *d*, at time zero (*a*) and time 11 yr (*b*) of a solar magnetic cycle.

The results of these computations are shown in Figs 1 and 2. Figure 1*a* and *c* shows the projection onto the solar equatorial plane (*XY*-plane) of the instantaneous positions of population particles arising from three streams which differ only by a separation of 10 AU in the initial value of their *Y* coordinate. Figure 1*b* and *d* shows the instantaneous positions in the *XZ*-plane of particles arising from three streams with $Y=0$. One stream is initially directed towards the Sun and the other two lie parallel to and 10 AU on either side of that direction. The sequence of points belonging to a stream corresponds to positions of particles which differ by 2 yr from the initial time when each particle was introduced at the boundary of the solar wind cavity. Figure 1*a* and *b* shows the instantaneous positions of all the particles at a time corresponding to the beginning of the solar magnetic cycle. Figure 1*c* and *d* repeat this information for a time 11 yr into the solar magnetic cycle. The contrast between *a*, *b* and *c*, *d* clearly demonstrates the decisive influence of the solar magnetic cycle on the distribution of the grains. The streams are diverted towards the *X*-axis in Fig. 1*a* and away from that axis in Fig. 1*c*. Figure 1*b* shows that when the solar dipole field axis points north, the grains are diverted from the solar equatorial plane, mainly due to the action of the electrical part of the Lorentz force. The grains are concentrated towards this plane when the solar dipole field points south (Fig. 1*d*). Some 3 to 4 AU ahead of the Sun the streams cross the equatorial plane, creating an enhancement in the number density. The grains behind the Sun experienced the oppositely directed magnetic field of the first half of the solar magnetic cycle as they entered the solar wind cavity, thus creating a depletion zone in the wake of the Sun.

Our computations are almost insensitive to whether the reversal of the direction of the interplanetary magnetic field is instantaneous or whether it is as gradual as a sine function. These results are based on a simple dipole field where higher order multipole or asymmetrical magnetic fields are ignored.

In Fig. 2*a* and *b* additional streams, projected in the *XZ* plane, are introduced higher in latitude than the streams in Fig. 1*b* and *d*. Figure 2*a* shows a concentration of particles developing along a line $X \approx -20$ AU, $Z \approx \pm 10$–20 AU (peaked around $\phi = 180°$). There is also a depletion zone of radius ≈20 AU surrounding the Sun. The deviation from the *XZ*-plane is ≤ ± 0.1 AU. The value of Q_{pr} used in the calculation is 0.4, which might be increased by surface roughness; however, this value decreases for elongated particles. The overall effect of increasing the radiation pressure efficiency Q_{pr} of the grains from 0.4 to as much as 1.0 ($\beta = 3.25$) is to move the concentration in Fig. 2*b* ≈3 AU along the positive *X*-axis. On the other hand, a decrease in the value of Q_{pr} has a negligible effect. The smaller bare grains that enter at low and medium heliocentric latitudes are essentially trapped around the solar wind magnetic field lines, and they are swept out near the solar wind cavity.

We have extended the study of the dynamics of interstellar grains to particles having radii of 0.12 and 0.005 μm streaming into the Solar System and included the effects of the solar dipole field's change of direction during the solar magnetic cycle. Additional forces on the particles such as Coulomb drag and solar wind ion pressure are less important than the Lorentz force. Particle trajectory computations show that an enhancement of the order of 50 or more in the number density of interstellar core-mantle particles may occur some 3–4 AU ahead of the Sun and close to the solar equatorial plane during yr 8–17 of the solar magnetic cycle. During the rest of the cycle, concentrations develop some 20 AU away from the Sun, while a depletion zone of ≈20 AU in radius surrounds the Sun.

As particle configuration varies strongly with the solar magnetic cycle, its effect must be taken into account in any treatment of this problem. Note that even grains with $\beta > 1$ will penetrate deep inside the Solar System during part of the solar magnetic cycle.

Subsequent computations may predict more precisely the directions and times to search for an interstellar component of the zodiacal cloud. Note that during the Solar Polar Mission (mid and late 1980s), concentrations of interstellar grains are expected (Figs 1*d*, 2*b*) which will offer a unique opportunity to detect the presence of interstellar grains in the Solar System[12].

We thank Drs J. M. Greenberg, J. R. Jokipii, E. H. Levy, K. F. Ratcliff and J. L. Weinberg for helpful comments, and Dr R. T. Wang for helpful discussions relating to radiation pressure efficiencies. This research was partially supported by the Planetary Atmospheres program of the NASA under grant NSG 7093.

Received 30 April; accepted 4 September 1979.

1. Weller, C. S. & Meier, R. R. *Astrophys. J.* **193**, 471 (1974).
2. Bertaux, J. L. *et al. Astr. Astrophys.* **46**, 19 (1976).
3. Bertaux, J. L. & Blamont, J. E. *Nature* **262**, 263 (1976).
4. Alvarez, J. M. *IAU Colloq.* No. 31 (1975).
5. Levy, E. H. & Jokipii, J. R. *Nature* **264**, 423 (1976).
6. Greenberg, J. M. & Hong, S. S. *IAU Symp.* No. 60 (eds Kerr, F. J. Simonson, S. C., III) (Reidel, Dordrecht, 1973).
7. Soumer, A. H. *Photoemissive Materials* (Wiley, New York, 1968).
8. Pierce, D. T. & Spicer, W. E. *Phys. Rev. Lett.* **27**, 1217 (1971).
9. Svalgaard, L., Wilcox, J. M. & Duvall, T. L. *Solar Phys.* **37**, 157 (1974).
10. Levy, E. H. *Nature* **261**, 394 (1976).
11. Schulz, M. *Astr. Space Sci.* **24**, 371 (1973).
12. Greenberg, J. M. & Schuerman, D. W. *Nature* **275**, 39 (1978).
13. Gustafson, B. Å. S. & Misconi, N. Y. *Bull. AAS* **10**, 653 (1978).

EVIDENCE THAT THE PROPERTIES OF INTERPLANETARY DUST BEYOND 1 AU ARE NOT HOMOGENEOUS

Donald W. Schuerman
Space Astronomy Laboratory
State University of N. Y. at Albany
Albany, N. Y. 12203

ABSTRACT

Traditionally, earth-based observations of the zodiacal light (ZL) require two assumptions for further analysis: (A1) the dust density (n) is a power of heliocentric distance (R), $n \propto R^{-\nu}$; (A2) the nature (scattering cross section, σ) of the dust is independent of location, $\sigma(r,h,\theta)=\sigma(\theta)$. Observations from Pioneer 10 do *not* verify these assumptions.

Both two-dimensional inversion techniques (Schuerman, 1979a) and more traditional methods of analysis (Hanner *et al.*, 1976) have been performed on portions of the ZL observations made from Pioneer 10/11 spacecraft. In developing the three-dimensional form of the ZL inversion (Schuerman, 1979b; henceforth called Paper I), it was realized that this more general technique should be applied to the Pioneer data because the velocity vectors of the spacecraft were not confined to the ecliptic plane. The previously mentioned analyses examined data with viewing directions parallel to the ecliptic; the three-dimensional inversion requires viewing along a great circle (see Fig. 1) containing (1) the line (η) which is both normal to the observer-Sun line and parallel to the ecliptic and (2) the spacecraft velocity vector (S). This great circle is called the inversion plane in Paper I where its geometric construction and the notation used here are defined in more detail. The angle ϕ is the inclination of the inversion plane to the ecliptic, and viewing in the direction of η

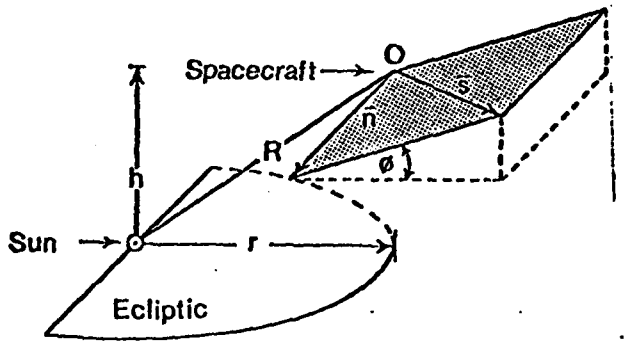

Fig. 1. Definition of the inversion (shaded) plane; it is normal to the r,h plane and contains S, the direction of motion of the spacecraft.

THE SYMMETRY PLANE OF THE ZODIACAL CLOUD NEAR 1 AU

Nebil Y. Misconi
Space Astronomy Laboratory
State University of N. Y. at Albany
Albany, N. Y. 12203

ABSTRACT

Analysis of zodiacal light observations from Mt. Haleakala, Hawaii show that the symmetry plane of the zodiacal cloud near 1 A.U. is close to the invariable plane of the solar system. Since the symmetry plane of the inner zodiacal cloud is close to the orbital plane of Venus (Misconi and Weinberg, 1978; Leinert *et al.*, 1979), we suggest that the symmetry plane changes inclination with heliocentric distance.

INTRODUCTION

The location in space of the plane of maximum dust density (symmetry plane) of the zodiacal cloud has important implications for the dynamics of solid particles in the solar system. These implications are related to questions such as the gravitational perturbations of the planets on the dust, the effects of solar magnetic forces, and the general dynamical history of dust ejected from comets. Helios 1 and 2 zodiacal light measurements near the region of 1 A.U. (Leinert *et al.*, 1979) find that the symmetry plane in this region has an inclination $i = 3 \pm 0.3°$ and ascending node $\Omega = 87 \pm 4°$, which is different from that of the invariable plane of the solar system ($i = 1.6°$, $\Omega = 107°$). At the same time, ground-based observations at Tenerife in the Canary Islands (Dumont and Sanchez, 1968) and satellite observations from the satellite D2B (Dumont and Levasseur-Regourd, 1978) find the symmetry plane close to the invariable plane near 1 A.U.

In the present study an attempt is made to obtain additional data on the location of the symmetry plane near the Earth's orbit using ground-based observations of the zodiacal light from Mt. Haleakala, Hawaii taken by Weinberg and Mann (1967).

THE OBSERVATIONS

Two nights of observations were found to be suitable for this

BRIGHTNESS AND POLARIZATION OF THE ZODIACAL LIGHT: RESULTS OF FIXED-POSITION OBSERVATIONS FROM SKYLAB

J. L. Weinberg and R. C. Hahn
Space Astronomy Laboratory
State University of N. Y. at Albany
Albany, N. Y. 12203

ABSTRACT

In an earlier paper Sparrow *et al.* (1976) found the polarized brightness of zodiacal light to have solar color at five sky positions for which there were fixed-position observations from Skylab: north celestial pole, south ecliptic pole, vernal equinox, and two places near the north galactic pole. The brightness and degree of polarization of zodiacal light at these sky positions are derived using Pioneer 10 observations of background starlight from beyond the asteroid belt (Weinberg *et al.*, 1974; Schuerman *et al.*, 1976) and the assumption that the zodiacal light is also solar color in total light.

Ten-color observations of sky brightness and polarization were made of portions of the antisolar hemisphere from Skylab (Weinberg *et al.*, 1975; Sparrow *et al.*, 1977). Three independent quantities were determined directly from the measurements: total brightness (B_t), polarized brightness (B_p), and orientation of the plane of polarization (χ), the last more precisely referred to as azimuth of vibration. These three quantities are related to the Stokes parameters I, Q, and U, respectively.

Except in regions relatively close to the Milky Way, the observed direction and amount of polarization (χ,B_p) in these space measurements can generally be attributed entirely to zodiacal light. To isolate the zodiacal light brightness, it is necessary to remove the brightness contribution of all discrete or "resolved" stars in each 6° diameter field of view (FOV) and to subtract the background starlight (integrated starlight, diffuse galactic light, light from extragalactic sources). Thus, the zodiacal light total brightness (B_z) is obtained as the residual after a several-step subtraction process. This subtraction process has been the largest single source of error in determining the brightness of zodiacal light in observations from space and, even more so, in observations from the ground.

Skylab observations included sky-scanning and fixed-position measurements, the latter at the north celestial pole, south ecliptic pole, and vernal equinox, and at two positions near the north galactic pole. A number of sequences of filters (Table 1) were used to observe these

THE EFFECT OF RADIATION PRESSURE ON THE RESTRICTED THREE-BODY PROBLEM

Donald W. Schuerman
Space Astronomy Laboratory
State University of N. Y. at Albany
Albany, N. Y. 12203

ABSTRACT

The classical restricted three-body problem is generalized to include the force of radiation pressure and the Poynting-Robertson effect. The positions of the Lagrangian points L_4 and L_5 are found as functions of β, the ratio of radiational to gravitational forces. The Poynting-Robertson effect renders the L_4 and L_5 points unstable on a time scale (T) long compared to the period of rotation of the two massive bodies. For the solar system, T is given by $T \approx [(1-\beta)^{2/3}/\beta]\ 544\ a^2$ yr where a is the separation between the Sun and the planet in AU. Implications for space colonization and a mechanism for producing asymmetries in the interplanetary dust complex are discussed; testing the latter may be possible from the Zodiacal Light/Background Starlight Experiment aboard the International Solar Polar Mission spacecraft to be launched in 1983.

A steady state solution of the motion of a β particle (a particle whose surface to volume is such that the force of radiation pressure is non-negligible) in the gravitational field of two larger, orbiting bodies of masses M_1 and M_2 is sought. It is assumed that M_1 and M_2 are in circular orbits about their common center of mass, that their angular frequency (Ω) is given by $\Omega^2 = G(M_1 + M_2)/a^3$, and that the β particle remains in the plane in which M_1 and M_2 revolve. In the rotating reference frame whose origin is the center of mass and whose angular frequency is Ω, the two components of the equation of motion of a β particle with coordinates (X,Y) are

$$\frac{\ddot{X}}{\Omega^2} - \frac{2\dot{Y}}{\Omega} = X - \frac{(1-\beta_1)\mu(X+\mu-1)}{r_1^3} - \frac{(1-\beta_2)(1-\mu)(X+\mu)}{r_2^3} \qquad (1)$$

$$\frac{\ddot{Y}}{\Omega^2} + \frac{2\dot{X}}{\Omega} = \left(1 - \frac{(1-\beta_1)\mu}{r_1^3} - \frac{(1-\beta_2)(1-\mu)}{r_2^3}\right)Y \quad . \qquad (2)$$

THE RESTRICTED THREE-BODY PROBLEM INCLUDING RADIATION PRESSURE

Donald W. Schuerman

Space Astronomy Laboratory,
State University of New York at Albany
Albany, N. Y. 12203

ABSTRACT

The classical restricted three-body problem is generalized to include the force of radiation pressure and the Poynting-Robertson effect. The positions of the Lagrangian points L_4 and L_5 are found as functions of β, the ratio of radiational to gravitational forces. The Poynting-Robertson effect renders the L_4 and L_5 points unstable on a time scale (T) long compared to the period of rotation of the two massive bodies. For the solar system, T is given by $T \approx [(1-\beta)^{2/3}/\beta]\ 544\ a^2$ yr where a is the separation between the Sun and the planet in AU. Implications for space colonization and a mechanism for producing azimuthal asymmetries in the interplanetary dust complex are discussed; the latter can be observationally tested by the Zodiacal Light Experiment aboard the International Solar Polar Mission spacecraft to be launched in 1983.